

Dependence of Critical Temperature and Resistivity of Thin Film Nb47wt%Ti on Magnetron Sputtering Conditions*

C. D. Hawes, L. D. Cooley, and D. C. Larbalestier

Applied Superconductivity Center, University of Wisconsin, Madison, Wisconsin, USA

Abstract—Niobium-titanium multilayers generally have depressed critical temperature, T_c . In this paper the variation of T_c and resistivity of magnetron sputtered Nb47wt%Ti thin films is studied as a function of the cathode power and target usage. The data are compared with analyses by Auger and scanning electron microscopy. Films made using a new target have properties which are similar to those of bulk Nb47wt%Ti when high cathode power is used. The data indicate a transition in the morphology of the film as power increases, which affects the rate at which interstitial atoms are incorporated into the growing film. After the target lost ~50% of its mass and acquired strong surface relief, bulk properties could not be obtained, because deposition rates for a given cathode power were lower than before. A small Ti enrichment (3-5%) between the films and the target was found for both sets of films.

I. INTRODUCTION

Thin film multilayers are ideal model systems to address questions about the ultimate limit of flux pinning in superconductors. Recent work has focussed on modeling Nb-Ti artificial pinning center wires [1]-[3], because their critical current density J_c exceeds 4000 A/mm² at 5 T and 4.2 K [4], [5] when Nb is used as the pin. Since many different metals can be used as flux-pinning centers, it has been proposed [6] that much stronger pinning and higher J_c might be attained if a better pin than Nb were used. The relative simplicity of multilayer experiments makes exploration of different possibilities, in principle, easier.

In order to thoroughly understand the influence of geometry in pinning center efficiency, it is very desirable to reproduce bulk properties in thin film multilayers, so that they can be better compared with wires, where pins have no long range geometrical texture. Reproducing bulk properties in transition metal films is generally difficult, however, due to the variety of parameters involved in sputter deposition. The sometimes uncontrollable variation of parameters can result in changes in structure and morphology from one film to another, which creates properties which are different from the desired bulk, or other, properties. Thus an important first step is to determine how the sputtering parameters affect the properties of the growing film. One important variable is the sputtering power, because this affects the gas density near the cathode and, thus the scattering of reflected neutrals and sputtered atoms leaving the target [7]. The power also affects the energy with which the sputtered atoms and gas atoms arrive at the substrate, thus affecting the grain size of the film, the amount of incorporated working gas and background gas,

and the overall composition of the film.

The influence of sputtering power on the properties of Nb47wt%Ti films is investigated in this paper. A set of films was made with cathode power between 175 and 300 W, and their superconducting and normal-state properties were characterized. The data suggest that a crossover in film morphology occurs, and, because this affects the amount of trapped gas, O or Ar, in the film, the resistivity and the critical temperature are also affected. During the course of this and other experiments, significant erosion of the sputter target was observed. Changes in the shape of the sputtering target, shown in Fig.1, with use cause significant variations in film properties. To address this issue, a second set of films was produced for the same power range as the first set. These films exhibited very different properties for a given cathode power than the first set. By gaining a better understanding of how sputtering parameters, especially the cathode power, and erosion affect the behavior of Nb47wt%Ti thin films, it is hoped that bulk properties can be made routinely in multilayers. We were able to obtain near - bulk properties under high deposition rates with new uneroded targets.

II. EXPERIMENT

All of the films examined in this paper were deposited by DC magnetron sputtering of a 5 cm diameter Nb46.5wt%Ti (Nb62.8at.%Ti) alloy target, derived from a Teledyne Wah Chang ingot. Its compositional variation was reported to be ± 1 wt.%.

The films were deposited on glass slides mounted 5.5 cm from the target. The slides were cleaned with a commercial glass cleaner, then ultrasonically rinsed in deionized water, and finally rinsed with acetone before being mounted in the vacuum chamber. The films were deposited after reaching a base pressure of ~ 10 μ Pa in a diffusion-pumped system with a liquid nitrogen trap. This pressure was achieved after getter-sputtering a pure Ti or the Nb47wt%Ti target for 5-10 minutes with the substrates shielded. The deposition of the films used 0.66 Pa of Ar flowing at a rate of 10 sccm.

A four-point measurement was used to determine the resistivity, ρ , of the films. Current paths were defined using a



Fig. 1. Approximate shape of the target cross section during the fabrication of the first set of films (left) and the second set (right). Target relief is represented in the right sketch. It is caused by the toroidal shaped magnetic field that holds the plasma near the target. This is characteristic of circular planar magnetrons. Contour lines represent field lines from the cathode magnets.

Manuscript received September 15, 1998

This work is supported by the U.S. Department of Energy under contract number DE-FG02-ER40961 and also benefits from facilities supported by the NSF-MRSEC (DMR-9632527)

150 μm wide bridge for the first set and a 60 μm wide bridge for the second set. These bridges were 3 mm long. The bridges were patterned by standard lithographic techniques and wet etching by a 50/50 solution of HF and HNO_3 . The amount of undercutting was found to be minimal after checking several films by SEM and light microscopy. The film thickness and the bridge width were measured using a Tencor Alpha-Step 200 Profilometer and verified by light microscopy and SEM.

Critical temperature T_c measurements were made using a SQUID magnetometer. Two values for T_c are reported, corresponding to a sample moment equal to 10% and 90% of the saturated 4.5K moment. The T_c measurements were made in a 10 Oe field while warming. The field was applied after the sample was cooled to 4.5 K in zero field.

Semi-quantitative compositional analyses of the films were performed in a PHI-660 scanning Auger probe and a LEO-982 FESEM. Two samples from each of the films sets were analyzed using both EDX and Auger electron spectroscopy (AES). Modeling software for electron trajectories in materials was applied to determine if there was any interaction with the substrate, due to the thickness of the samples being $<1 \mu\text{m}$, for the EDX analysis. This revealed that there was little substrate interaction, since a relatively low beam energy of 10 keV was used and the film thickness was between 522 nm and 740 nm. The AES depth profiling consisted of taking a surface scan, and then performing an alternating routine of sputtering for 30 seconds, waiting for 10 seconds, taking spectra, and repeating. The total sputtering time was 10 minutes.

III. RESULTS

Fig. 2 shows that both film sets exhibit a nearly linear relationship between cathode power and deposition rate. The film set, made with the target after severe erosion has occurred, shows a significant decrease in deposition rate for any given power. Above 300 W, a significant heating of the target occurred, leading to a time dependent cathode voltage for a fixed power.

The critical temperature is shown in Fig. 3. The film set made with the flat target, shown as closed symbols in Fig. 3, exhibits a steady increase in T_c and a more narrow T_c transition with increasing power. By contrast, the film set made with the target after severe erosion shows a slight decrease in T_c with increasing power and a scattering of the transition. The highest value of T_c is 8.8 K, relatively close to the bulk value of Nb47wt%Ti, 9.1K. Resistive measurements gave a transition to zero resistance at 8.95 K for this film.

The resistivity data is presented in Fig. 4. The film set made with the target flat shows an increase in ρ from 78 $\mu\Omega\text{-cm}$ at 175 W to 97 $\mu\Omega\text{-cm}$ at 250 W, at which point ρ sharply decreases to 74 $\mu\Omega\text{-cm}$ at 275-300 W. The film set made with the target after severe erosion shows a steady decrease of ρ from 98 $\mu\Omega\text{-cm}$ at 175 W to 83 $\mu\Omega\text{-cm}$ at 275 W. All of the resistivity values are higher than of bulk Nb47wt%Ti, 65 $\mu\Omega\text{-cm}$. Table 1 contains the EDX data and Table 2 contains

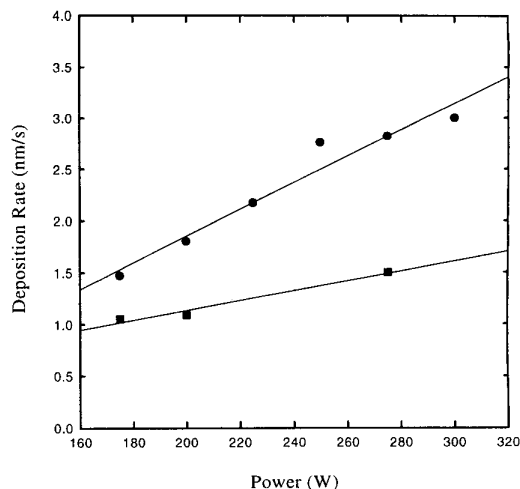


Fig. 2. Deposition rate as a function of power for the films made when the target was flat, represented as circles, and after the target had been severely eroded, represented as squares.

the AES data, both before and after depth profiling. Although the EDX and AES data are not in detailed quantitative agreement with each other, they are both in agreement that the film is always enriched in Ti by 2-5% regardless of power or the amount of target erosion.

IV. DISCUSSION

There are two effects apparent in the data. First, changes in the cathode power and the deposition rate cause different properties in the thin films. Second, films made at a given

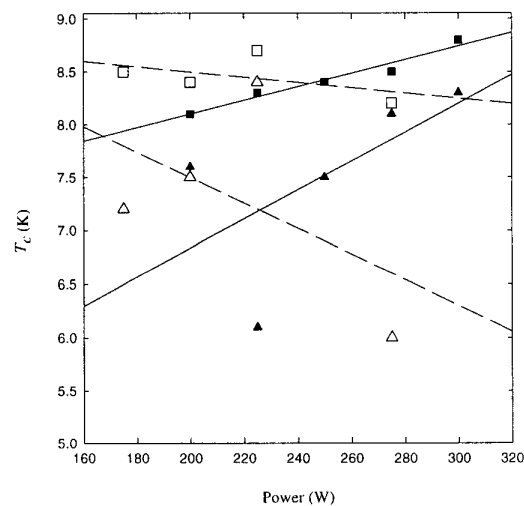


Fig. 3. T_c as a function of power for both film sets. Closed symbols represent films made when the target was flat and open symbols represent films made when the target was severely eroded. Squares are 90% m_{sat} and triangles are 10% m_{sat} .

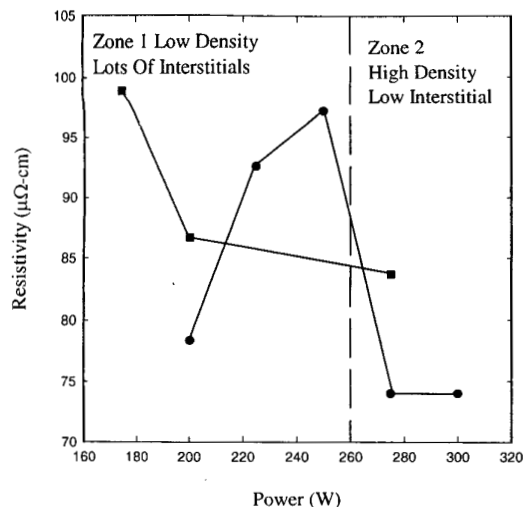


Fig. 4. Room temperature resistivity as a function of sputtering power for both film sets. Circles represent films made when the target was flat and squares represent films made when the target was severely eroded.

cathode power have different properties for a different target age.

The effect of the different target conditions can be assessed in terms of the lower deposition rate [8], as will be discussed later, but to keep the discussion simple the two film sets will be discussed separately.

The film set made when the target was flat shows increasing T_c and a sharper T_c transition with increasing power. The sharper transition indicates better homogeneity in the films. This transition may arise from higher film bombardment by energetic particles for a higher cathode power. At low cathode powers the gas density near the cathode is high, which increases the scattering of energetic neutrals and sputtered atoms [7]. This causes a decrease in the energy and number of particles that bombard the substrate, leading to a Zone 1 structure in the film [9]-[11]. This structure typically has low density and columnar grains, and fairly large amounts of oxygen or other impurities can be trapped. Table 2 shows higher surface concentrations of oxygen in the films grown at low power, and AES depth profiling indicates that oxygen concentrations of a few percent are maintained well into the film. By contrast, bombardment of the substrate is increased both by the power increase and the decrease in scattering near the cathode, due to a lowered gas density near the cathode caused by cathode heating [7]. The bombardment of the films by more particles with higher energy per particle leads to a different morphology, the so called Zone 2 structure, [9]-[11], which is characterized by a high number of columnar grains and higher film density. The denser film is less susceptible to interstitial

TABLE 1
RESULTS OF EDX ANALYSIS OF FILM SET 1, FILM SET 2, AND THE TARGET

Film Set 1		Film Set 2		Target
Power (W)	Ti (at%)	Power (W)	Ti (at%)	Ti (at%)
200	64.9	200	66.1	61.4
275	65.8	275	64.9	

incorporation and exhibits more homogeneous properties [11]. Indeed, the higher power films had a sharper T_c transition and higher T_c .

The abrupt drop in resistivity at about 250 W can be interpreted as a change from a Zone 1 to a Zone 2 structure. The Zone 1 structure typically has higher resistivity than the Zone 2 structure. Reference [12] points out that the transition from low to high resistivity is a fairly steep function of the working gas pressure. Changes in working gas pressure at constant power have been shown to produce similar results as changes in power at constant pressure [7]. This is consistent with a correlation between the resistivity and the amount of trapped gas. The reason for T_c being somewhat lower than the bulk, even at high power, may have to do with Ar incorporation into the film. It has been shown that the oxygen content in molybdenum films decreased and Ar content increased to about 1% at 1 nm/s deposition rates, above which the Ar concentration appeared to saturate [13]. Unfortunately, we have not yet been able to do the AES depth profiling with Xe gas, so that we can detect trapped Ar.

The differences in the Nb-Ti film composition from that of the target can be attributed to the different emission profiles of Nb and Ti. Ti has a lower mass than Nb, so the emission of Ti atoms is more perpendicular to the target. The plume of sputtered Ti atoms thus extends over a smaller solid angle than does the plume of sputtered Nb atoms, leading to a higher concentration of Ti in the film than if the substrate is sufficiently far from the target, consistent with the data of Table 1 and Table 2.

The overall lower T_c values and higher resistivity values in the film set made after the target was severely eroded can be attributed to the change in the shape of the target due to sputter erosion. Fig. 2 shows that films made with the target after being severely eroded have lower deposition rates than those made when the target was still flat, at the same power. Reference [8] has shown that plasma density increases with

TABLE 2
RESULTS OF AES ANALYSIS OF FILM SET 1, FILM SET 2, AND THE TARGET

Before depth profiling					
Film Set	Pwr (W)	O(at%)	C (at%)	Ti (at%)	Nb (at%)
Film Set 1	200	58.9	13.0	23.3	4.80
	275	40.0	42.4	15.8	1.80
Film Set 2	200	60.6	17.9	18.3	3.20
	275	51.0	16.8	21.7	10.5
Target		40.0	45.0	10.2	4.80
After depth profiling					
Film Set	Pwr(W)	O(at%)	C (at%)	Ti (at%)	Nb (at%)
Film Set 1	200	2.00	2.50	54.1	41.4
	275	2.00	3.50	50.2	44.4
Film Set 2	200	4.00	6.00	49.0	41.0
	275	5.00	3.00	48.9	43.1
Target		3.00	3.50	47.3	46.2

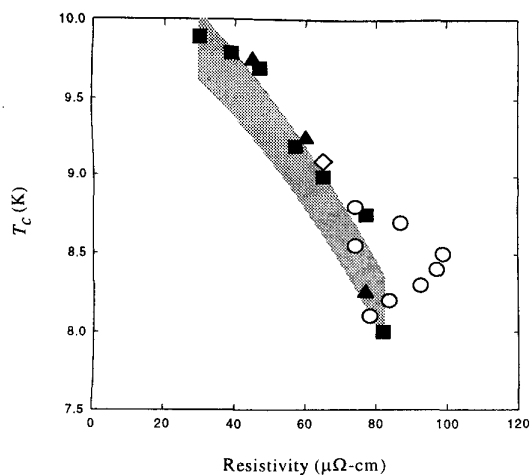


Fig. 5. Critical temperature as a function of resistivity. Films made when the target was flat and severely eroded represented by open circles, closed squares are the data of [14], closed triangles are the data of [15], and the open diamond represents the sputtering target.

target erosion. The increase in plasma density would then lead to an increase in scattering, and lower deposition rates at all power settings. Thus, films made when the target was heavily eroded should display properties similar to the films made when the target was flat and at lower powers. However, since the threshold for Zone 2 is at a deposition rate of ~ 2.8 nm/s, Zone 1 forms even at the highest power setting for the eroded target. The films made when the target was severely eroded have overall higher resistivity, and AES data shows that these films have a surface oxygen content similar to or higher than that of the films made at low power with the flat target. The AES data also indicates that the oxygen content of films made when the target was severely eroded does not drop below that of the films made when the target was flat.

The films from the second set displayed visibly higher stress than films from the first set. Films from the first set displayed no wrinkling, characteristic of films under large amounts of compressive stress, or peeling, characteristic of films under high tension. Films from the second set sometimes displayed catastrophic compressive stress, characterized by lifting entirely off the substrate. We think that the combination of the more open Zone 1 structure and adsorbed water on the substrate (due to humidity and other factors) resulted in the films experiencing a large amount of stress. Films made with a new target under similar humidity conditions displayed no visible effects. This is another indicator of how cathode power and changes in the target surface affect the behavior of films.

The films are compared to NbTi bulk alloys made by [14] and [15] in Fig. 5, to assess how close we can come to the quality of the bulk alloy. In Fig. 5, the gray region represents the range of bulk properties of [14] and [15]. The AES and EDX data suggest an enrichment in Ti by 2-5% relative to the target composition. This should lead to decreasing T_c and increasing resistivity. Both are seen. However, most samples fall out of the gray region, suggesting interstitial / contamination effects, too. It is clear that films made at a high

rate from a flat target display properties which are close to those of bulk alloys.

V. CONCLUSIONS

Two sets of magnetron-sputtered Nb47wt%Ti films were made over a range of cathode power. One set was made using a new target with a flat surface, and the other after the target had become eroded by sputtering and had developed contours and surface relief. The T_c and resistivity of these films were measured, and their compositions analyzed, to determine the quality of these films. Films made at high power using a flat target displayed properties close to bulk alloys. Those that were grown at either lower sputtering power or after extensive target use displayed higher resistivity and lower T_c . The improvement of film properties with power is due to an increase in the homogeneity of the deposited film and a transition in its growth morphology from a low to a high density columnar structure.

ACKNOWLEDGMENT

We would like to thank P. Lee, J. Jacobs, and R. Noll for assistance in performing the microscopy. Discussion and assistance by A. Squitieri, M. Naus, and K. Pierson is gratefully acknowledge,

REFERENCES

- [1] E. Kadyrov, A. Gurevich, and D.C. Larbalestier, *Appl. Phys. Lett.*, vol. 68, pp. 1567-1569, 1996.
- [2] J.D. McCambridge et al., *IEEE Trans. Appl. Supercond.*, vol. 7, pp. 1134-1137, 1997.
- [3] W. H. Warnes, K. Faase, and J. A. Norris, *Adv. Cryo. Eng. (Materials)*, vol. 42B, pp. 1143-1150, 1996.
- [4] R.W. Heussner, J.D. Marquardt, P.J. Lee, and D.C. Larbalestier, *Appl. Phys. Lett.*, vol. 70, pp. 901-903, 1997.
- [5] K. Matsumoto et al., *Appl. Phys. Lett.*, vol. 64, pp. 115-117, 1994.
- [6] L.D. Cooley, P.J. Lee, and D.C. Larbalestier, *Phys. Rev. B*, vol. 53, pp. 6638-6652, 1996.
- [7] S.M. Rosnagel, I. Yang, and J.J. Cuomo, *Thin Solid Films*, vol. 199, pp. 59-69, 1991.
- [8] K. Ichihara, K. Tateyama, R. Sakai, and T. Ishigami, *IEEE Trans. Magn.*, vol. 6, pp. 4450-4451, 1997.
- [9] C. Hudson and R.E. Somekh, *J. Vac. Sci. Technol. A*, vol. 14, pp. 2169-2174, 1996.
- [10] D.W. Hoffman and J. A. Thorton, *Thin Solid Films*, vol. 40, pp. 355-363, 1977.
- [11] M. Ohring, *The Materials Science of Thin Films*. San Diego, Calif.: Academic Press, Inc., 1992.
- [12] J.A. Thorton and D.W. Hoffman, *J. Vac. Sci. Technol.*, vol 14, pp. 164-168, 1977.
- [13] D.W. Hoffman, "Stress and Property Control In Sputtered Metal Films Without Substrate Bias," *Thin Solid Films*, vol. 107, pp. 353-358, 1983.
- [14] D.L. Moffat, *Phase Transformations In the Titanium-Niobium Binary Alloy System*. Ph.D. thesis, University of Wisconsin, 1983.
- [15] D.G. Haworth, *The Upper Critical Field and High Field Critical Current of Niobium-Titanium and Niobium-Titanium Based Alloys*. Ph.D. thesis, University of Wisconsin, 1984.